

Synthesis, Bulk, and Surface Characterization of Niobium-Doped Fe₂O₃ Single Crystals

C. SANCHEZ, M. HENDEWERK, K. D. SIEBER, AND G. A. SOMORJAI

*Department of Chemistry, University of California,
Berkeley, California 94720*

Received January 24, 1985; in revised form June 3, 1985

Single crystals of niobium-substituted α -Fe₂O₃ were grown by using chemical vapor transport with tellurium tetrachloride and were characterized by using bulk methods (X rays, resistivity, magnetism) and surface techniques (low-energy electron diffraction (LEED), Auger, X-ray photoelectron spectroscopy (XPS)). Niobium-substituted α -Fe₂O₃ crystallizes with the corundum structure, and is an extrinsic *n*-type semiconductor with a room temperature resistivity of approximately 85 Ω cm, and an activation energy for conductivity of 0.22 eV. Low-temperature susceptibility measurements suggest that the substitution of niobium(V) in octahedral sites leads to reduction of iron(III) to iron(II) without spinel phase inclusions. The main face of the single crystal platelets is the (001) basal plane of α -Fe₂O₃. The surface is very well ordered as shown by LEED. These crystals show good potential for application in both photoelectrochemistry and surface science studies. © 1986 Academic Press, Inc.

Introduction

The interesting catalytic and photoelectrochemical properties of iron oxide are linked to its behavior as a semiconductor (1, 2). Stoichiometric hematite, α -Fe₂O₃, is intrinsically an *n*-type semiconductor with a bandgap of 2.2 eV (3, 4) (visible light), but is an insulator at room temperatures ($R > 10^6 \Omega$ cm) (5, 6). Iron oxide is inexpensive, is extremely stable under acidic and basic aqueous conditions, and has useful optical properties (good matching between the bandgap and the solar spectrum and a large absorption coefficient).

It is possible to produce a less resistive semiconducting oxide material by reducing some of the iron(III) to the iron(II) state (7). Hematite is then a mixed valence compound with enhanced conductivity at room

temperature which is due to a hopping process of electrons between Fe²⁺ and Fe³⁺ ions (6). The Fe²⁺ can be introduced by producing oxygen deficiencies or by adding a dopant which induces a charge compensation process. However, the corundum α -Fe₂O₃ phase has a low solubility for M^{2+} ions since an Fe(III)_{2-x}Fe(II)_xO₃ stoichiometry induces the formation of the Fe₃O₄ spinel phase. Thus it is difficult to prepare homogeneous semiconducting samples of Fe₂O₃ in which semiconductive properties do not arise from Fe₃O₄ phase inclusions. It has been shown that it is possible to prepare ternary solid solutions of Fe₂O₃ with TiO₂ (8) and ZrO₂ (9) which are conducting and which do not contain spinel phase inclusions. We have recently synthesized germanium-doped Fe₂O₃ single crystals (10) which are also conductive without spinel

phase inclusions and which exhibit good photoelectrochemical properties. However, because the germanium ions are smaller than iron ions the germanium can either substitute for iron in an octahedral site in the iron oxide lattice or occupy an interstitial tetrahedral site. Kennedy *et al.* have shown that it is possible to dope iron oxide with niobium, in the form of sintered pellets, which do exhibit photoelectrochemical behavior (2). For this work we have chosen to dope single crystals of Fe_2O_3 with niobium. Because of the extended $4d$ orbitals niobium will be forced to occupy a substitutional octahedral site.

In this paper we report the preparation and characteristic properties of $\text{Fe}_{2-x}\text{Nb}_x\text{O}_3$ ($x < 2\%$) single crystals. We have prepared very high quality crystals by chemical vapor transport and have characterized them by bulk methods (X rays, magnetic susceptibility, electrochemistry) and surface analytical techniques (Auger, X-ray photoelectron spectroscopy (XPS), and low-energy electron diffraction (LEED)). It was found that Nb-substituted Fe_2O_3 crystallizes with the corundum structure and with no spinel phase inclusions. The crystals are large with surface areas of 5 to 35 mm^2 and thicknesses of 0.1 to 1 mm. Low-energy electron diffraction patterns were obtained from these crystals before cleaning or annealing the surfaces, which indicates that the crystal surfaces are very well ordered. They do not have reconstructed surfaces or ordered defects and contain very little carbon or other impurities. Very few studies have been carried out with the $\text{Fe}_{2-x}\text{Nb}_x\text{O}_3$ ternary system, yet we find that these materials are quite active as photoanodes and as materials to study photooxidation processes.

Experimental

Single crystals of niobium-substituted Fe_2O_3 were prepared by chemical vapor

transport using tellurium(IV) tetrachloride as a transport agent. Approximately 1 g of charge consisting of Fe_2O_3 (MCB reagent) with a 1 mole% of elemental niobium was placed in a 15 cm \times 13 mm-i.d. silica tube along with approximately 20 mg of Te metal. The tube was then evacuated to below 1 μm , backfilled with 400 Torr of chlorine gas, and then sealed. An identical procedure was used to prepare pure Fe_2O_3 crystals for comparison, except that the addition of niobium to the charge was omitted. The tubes were then placed in the zone transport furnace and after 24 hr of back transport from 900 to 800°C the charge was transported for 10 days. The temperature of the charge zone was 890°C and that of the growth zone 780°C. After 10 days the furnace was turned off and left to cool to room temperature. The tubes were then removed from the furnace, opened under vacuum, and the product washed with dilute nitric acid, rinsed with water, then dried with acetone. The 6 \times 5 \times 1-mm platelets shown in Fig. 1 were grown using this technique. The major face of the crystals, as determined by X-ray diffraction was the (001) basal plane.



FIG. 1. Photographs of Nb-doped iron oxide single crystal platelets 6 \times 5 \times 1 mm.

Bulk Characterization

X-Ray powder diffraction was performed on ground single crystal powders using a Siemens Model D500 powder diffractometer equipped with monochromated CuK α radiation. Fast scans were carried out using a scan rate of 6° 2 θ /min for phase identification. Slow scans for lattice parameter determination were carried out using a scan rate of 0.5° 2 θ /min and lattice parameters were calculated using a least-squares refinement technique with the aid of a computer. All cell parameters were calculated using hexagonal indexing, and all crystalline directions referred to hereafter are with reference to the hexagonal unit cell.

The electrical properties of samples were measured using the Van der Pauw (11) four-probe technique and all crystals were measured on the (001) basal plane. Contacts to the samples were made using an indium-gallium eutectic and the ohmicity of the contact was verified by repetitive measurement of the resistivity at several different magnitudes between 10 μ A and 100 mA. The variation of the electrical resistivity with temperature was measured using the same techniques except that the ohmic contacts were provided by ultrasonic soldering of pure indium metal. The carrier type of the conducting crystals was determined by qualitative measurement of the Seebeck voltage at room temperature.

The magnetic properties of ground single crystal powders were investigated using an S.H.E. Corporation "SQUID" susceptometer. The magnetic susceptibility of samples was measured at varying field strengths between 5 and 25 kG in the temperature region between 200 and 10 K to examine the field dependence of the sample susceptibility at various temperatures.

Surface Characterization

Surface analysis experiments were carried out in an ultra high vacuum chamber

with a base pressure of 2×10^{-10} Torr. The chamber is equipped with Physical Electronics instruments for LEED, XPS, Auger, and argon ion bombardment. The detector used was a double pass cylindrical mirror analyzer. First-order diffraction patterns (LEED) were obtained with an incident electron beam energy of 68 eV. XPS spectra were obtained using the K α X rays from a Mg anode as excitation radiation. The binding energies were measured with respect to the C(1s) peak which was assumed to be 284.5 eV. Auger analysis was performed using an incident electron beam of 2 keV energy and 1 mA emission current. The crystals were cleaned using Ar ion bombardment. The argon gas pressure was maintained at 5×10^{-5} Torr and the ion gun operated at 1.5 keV and 10 mA. Samples were sputtered for very short times in order to remove carbonaceous deposits without reducing the sample significantly. The crystals were annealed at $\sim 700^\circ\text{C}$ by resistively heating the tantalum foil on which the crystal was mounted.

Photoelectrochemical Measurements

The cyclic voltammetry measurements were carried out using a Pine RDE-3 potentiostat in a standard three-electrode configuration with a platinum counterelectrode and an SCE reference electrode in an all quartz cell. The illumination source was a 300-W tungsten halogen lamp. The light was passed through an IR filter to reduce heating of the sample. The intensity of the focused light as determined with a calibrated thermopile was approximately 30 mW/cm². The electrolyte was 1 M NaOH prepared using distilled deionized water and Mallenckrodt analytical grade NaOH pellets. Electrodes of niobium-substituted Fe₂O₃ were prepared by mounting the crystals on a copper plate with an indium-gallium eutectic to provide an ohmic contact. The copper plate was attached to a glass-

covered metallic lead, and the entire assembly was insulated with a silicon resin.

Results and Discussion

X-Ray Studies

The results of the crystal growth experiments show that Nb-substituted Fe_2O_3 can be grown under the same conditions as pure Fe_2O_3 . $\alpha\text{-Fe}_2\text{O}_3$ itself crystallized with the corundum structure which can be described as a hexagonal close-packed array of oxygen anions in which two thirds of the octahedral interstices are occupied by cations. X-Ray powder diffraction patterns of the Nb-substituted and pure ground single crystals indicated single phase corundum patterns in all cases. It was concluded that the niobium-substituted and pure materials are therefore isostructural. The major face of the single crystals was the (001) basal plane, and the least-squares lattice parameters determined for niobium-substituted Fe_2O_3 are $a = 5.033 \text{ \AA}$, $b = 13.74 \text{ \AA}$. These results are the same as those of pure Fe_2O_3 (12) and are in good agreement with several examples given for single crystals prepared by CVT (10, 13).

In order to determine the composition of the solid solution of niobium in the corundum lattice we have performed elemental analysis of the niobium-doped $\alpha\text{-Fe}_2\text{O}_3$ crystals using a scanning electron microscope equipped with a Kevex probe. These experiments show the presence of niobium at a concentration of approximately 1.4 at.%, which is very near the detection limit of the Kevex probe. These results suggest that the niobium concentration in our substituted crystals is around 2 mole% or less. This is in complete agreement with the phase diagram for $\text{Fe}_{2-x}\text{Nb}_x\text{O}_3$ ternaries, which indicates an $\alpha\text{-Fe}_2\text{O}_3$ solid solution of niobium at low concentration, less than $2 \pm 1\%$ (14). Moreover, ternary systems like $\text{Fe}_4\text{Nb}_2\text{O}_9$ also crystallize with the corundum structure (15), and this probably ac-

counts for the existence of a solid solution of niobium in the $\alpha\text{-Fe}_2\text{O}_3$ with conservation of the corundum structure. It is obvious that the apparent lack of change in the lattice parameters of the niobium-substituted Fe_2O_3 relative to the pure phase is due to the fact that only a very small amount of niobium was substituted into the lattice.

Electrical Properties

The room temperature resistivity of single crystals of $\text{Fe}_{2-x}\text{Nb}_x\text{O}_3$ ($x \sim 0.015$) is about $85 \pm 5 \Omega \text{ cm}$ while that of pure Fe_2O_3 crystals grown under the same conditions is greater than $10^6 \Omega \text{ cm}$. These values are in good agreement with values reported in the literature for Zr- and Ti-doped Fe_2O_3 (9, 16). The decrease in resistivity is explained by the substitution of iron(III) by niobium(V) in the corundum lattice which leads to a reduction of iron(III) to iron(II).

Qualitative measurements of the Seebeck voltage showed the Nb-substituted Fe_2O_3 to be an *n*-type semiconductor. Quantitative Seebeck experiments and electrical measurements carried out on doped Fe_2O_3 (5, 6) have shown that the mobility in these materials is thermally activated (5-7, 17) and that conductivity occurs via an electronic hopping between Fe(II) and Fe(III).

A plot of the logarithm of resistivity ($\Omega \text{ cm}$) versus $1/T$ for niobium-doped Fe_2O_3 is shown in Fig. 2. In the range of temperature (160 to 300 K) this curve follows an Arrhenius behavior. From the slope of this curve we can extract the activation energy of the conductivity which is about 0.22 eV. This value is consistent with those reported in the literature for materials based on iron oxide (7, 10). Assuming a mobility at room temperature of about $0.1 \text{ cm}^2 \text{ V sec}$ (17) for these materials, and taking their respective values of the resistivity ($R = 5 \Omega \text{ cm}$ for germanium-doped $\alpha\text{-Fe}_2\text{O}_3$, and $R = 85 \Omega \text{ cm}$ for niobium-doped $\alpha\text{-Fe}_2\text{O}_3$), this gives rise to the following carrier densities:

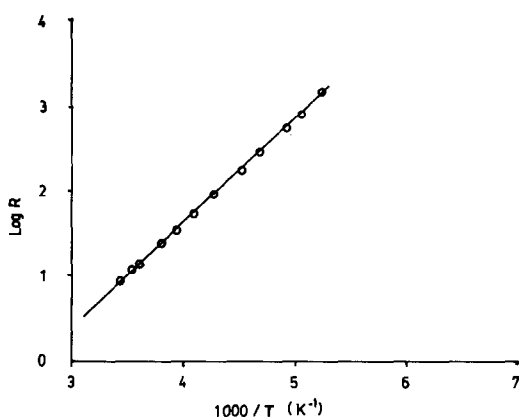


FIG. 2. Arrhenius plot of resistance as a function of temperature ($\log R$ vs $1/T$) for Nb-doped iron oxide single crystals.

$$N_D(\text{Fe}_{2-x}\text{Ge}_x\text{O}_3) = 1.25 \times 10^{19} \text{ cm}^{-3} \text{ and} \\ N_D(\text{Fe}_{2-x}\text{Nb}_x\text{O}_3) = 7.4 \times 10^{17} \text{ cm}^{-3}.$$

Magnetic Susceptibility

Although the X-ray diffraction patterns of the powdered single crystals indicate that the corundum structure is the only phase present, the possibility still exists that Fe₃O₄ phase inclusions below the detection limit of X-ray diffraction might be present. Fe₃O₄ inclusions in the Fe₂O₃ lattice can also produce an *n*-type semiconductor (18). The electrical conduction in that case would occur through a percolation of carriers provided by the spinel phase inclusions because Fe₂O₃ is a high resistivity material while Fe₃O₄ is a semimetal at room temperature (7). The presence of Fe₃O₄ phase inclusions in Fe₂O₃ can be detected by measuring the magnetic susceptibility of the material at various magnetic field strengths. If Fe₃O₄ phase inclusions were present in these materials a constant and dramatic field dependence on temperature should be observed. There would be no contribution to the magnetic field dependence from Fe₂O₃ because hematite is antiferromagnetically ordered in the temperature domain (10–200 K) studied.

A Honda–Owens plot representing the variation of magnetic susceptibility with reciprocal field strength for Nb-substituted Fe₂O₃ is presented in Fig. 3. The plot for Fe₂O₃ is shown in the same figure. The temperature range investigated is 10–200 K, well below the Curie temperature of Fe₃O₄. The Honda–Owens plot should exhibit a distinct positive slope if ferrimagnetic Fe₃O₄ inclusions are present in our materials. Two important observations can be made from these experiments. The first is that the magnitude of the magnetic susceptibility is the same in the Nb-substituted Fe₂O₃ as in the pure Fe₂O₃. The second is that our Honda–Owens plots exhibit slightly negative slopes, indicating a weakly antiferromagnetic coupling. From these observations we can conclude that the Nb-doped Fe₂O₃ single crystals are free of spinel phase inclusions and are homogeneous materials.

The magnetic properties of the Nb-substituted Fe₂O₃ are slightly different from those which we recently reported for Ge-substituted Fe₂O₃ (10). In the latter case the Honda–Owens plot exhibited almost constant but slightly positive slopes. This difference in magnetic properties may be due to differences in the substitutional nature of the Ge and Nb atoms in the corundum lattice. It is more probable that

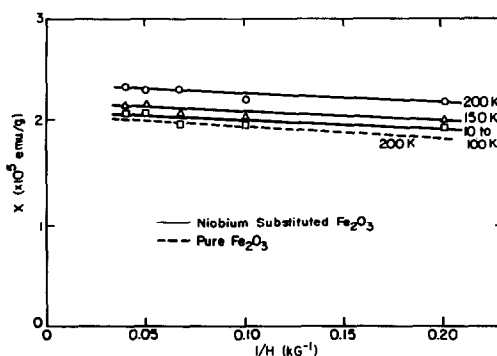


FIG. 3. Magnetic susceptibility vs $1/H$ for Nb-doped iron oxide single crystals.

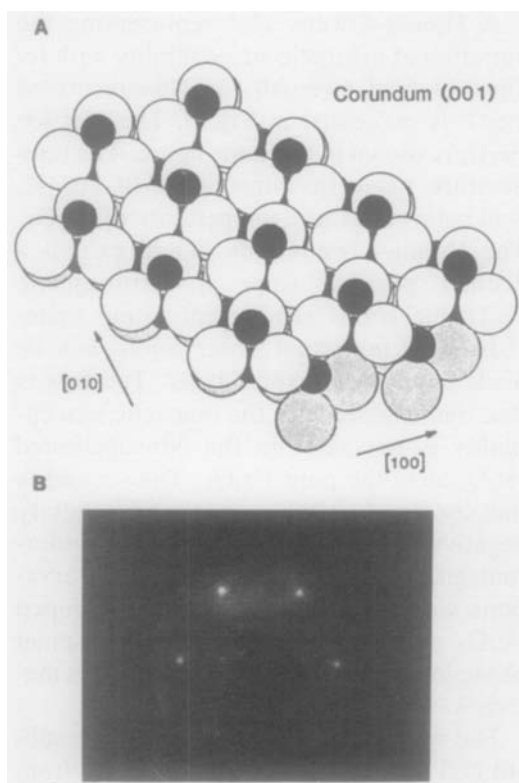


FIG. 4. (A) Model of the corundum (001) structure. The solid circles represent Fe^{3+} ions. The open circles are the first layer of O^{2-} ions, the shaped circles are the second layer of O^{2-} ions. (B) LEED pattern of the Nb-doped iron oxide single crystals. Beam energy of 102 eV.

niobium is really replacing an iron(III) atom in an octahedral site rather than occupying an interstitial tetrahedral site because Nb is a large ion with extensive $4d$ orbitals. This is supported by the experiment reported by Bertaut. He found, by using magnetic measurements and neutron diffraction, that niobium occupies the octahedral site in the corundum structures like $\text{Fe}_4\text{Nb}_2\text{O}_9$ (15). Germanium, on the other hand, is smaller than the Fe and would be expected to substitute in interstitial sites satisfying the tendency of smaller cations to favor tetrahedral coordination. It might be useful to perform experiments such as ESR to characterize the paramagnetic defects of doped

iron oxides in order to elucidate the exact role of the dopant in these materials.

Surface Characterization

In addition to the high purity and homogeneity of the Nb-doped crystals in the bulk, we have found that the crystal surfaces are also homogeneous and virtually free of defects or impurities directly after the preparation procedure. The major face of the crystals was determined to be the (001) basal plane by bulk X-ray diffraction. A pictorial representation of this hexagonal packed array of oxygen atoms with octahedrally coordinated iron atoms is shown in Fig. 4. A LEED pattern of the Nb-doped single crystals is also shown in Fig. 4. The hexagonal pattern is indicative of the (001) face as can be seen by the cross-sectional representation. This LEED pattern was obtained from the crystals, as received. The intensity of the diffraction spots was low but easily detectable. Auger analysis of the crystals showed that several monolayers of carbon are present on the freshly prepared surfaces which attenuates the intensity of the iron oxide crystal diffraction spots. After cleaning the sample with argon ion bombardment for several minutes and subsequently annealing the crystal to $\sim 700^\circ\text{C}$ for 10 min, no trace of carbon was seen by Auger. The LEED pattern became very sharp but did change, indicating that the surface was not reconstructed nor had any ordered defects occurred directly after preparation.

The Auger analysis of the samples before the argon ion bombardment showed the presence of oxygen, iron, niobium, carbon, and trace amounts of chlorine (from the charge in the transport). After cleaning the crystal, no impurities were detected. XPS spectra were used to quantitatively measure the relative amounts of iron, oxygen, and niobium. These results showed that Nb was present at the surface in amounts of $<1\%$, while the Auger peak to peak ratio of

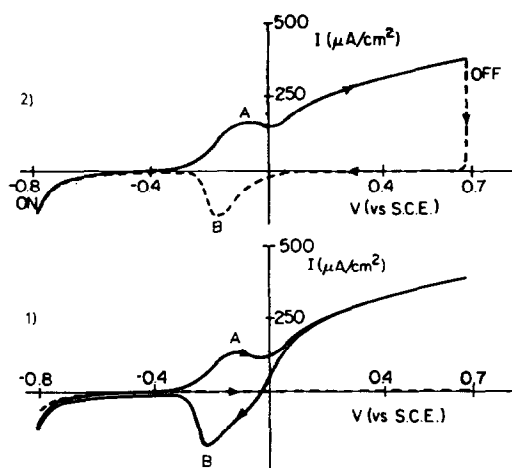


FIG. 5. Direct current voltammogram for Nb-doped iron oxide single crystals. The solid curves were obtained under illumination and the dashed curves in the dark: (1) continuous cycling in the dark and under illumination; (2) anodic sweep under illumination followed by cathodic sweep in the dark.

$\text{O}(510)/\text{Fe}(651)$ was 3.0 ± 0.2 in agreement with previous Auger studies (20).

Direct Current Voltammetry Experiments

Direct current voltammetry experiments were carried out as a simple test of the photoelectrochemical properties of the Nb-doped single crystals. They were performed on the (001) basal plane of the crystals in 1 M NaOH solution. The cyclic voltammograms observed under cathodic and anodic bias exhibited the characteristics of an ideal n -type semiconductor diode. The voltammograms measured in the dark showed very low dark currents, well below $1 \mu\text{A}/\text{cm}^2$ in the range between -1.0 and $+0.7$ V (SCE). Direct current voltammograms taken from crystals under the illumination of a tungsten halogen lamp showed photocurrents on the order of 500 to $700 \mu\text{A}/\text{cm}^2$ at $+0.4$ V (SCE) as shown in Fig. 5. These photocurrents are most likely due to photoinduced electrolysis of water. Continuous cycling experiments showed that these materials were stable under illu-

mination. There was no observable attenuation of the photocurrents and no visible tarnishing of the crystal surface.

The qualitative behavior of the single crystal electrodes is in good agreement with that of $\alpha\text{-Fe}_2\text{O}_3$ photoanode materials reported in the literature (2, 19–21), except that no photocathodic currents were ever observed at negative potentials (18, 21). There is an additional interesting feature which is observable in the cyclic voltammograms of these Nb-doped Fe_2O_3 crystals. These crystals exhibit a second photooxidation process which is depicted in Fig. 5 as wave A. When cycling the electrode from -1.0 to $+0.7$ V (SCE) with the light on, the photooxidation wave A appears. If the light is switched off as the cycling continues from $+0.7$ to -1.0 V, wave B appears—even under these dark conditions. If we start at the positive potential with the light on, before the potential at which wave B should appear, we do not obtain the reduction wave. But if we turn the light on as we continue the cycle, sweeping anodically, wave A appears. The redox potential at which this oxidation reduction process occurs is approximately -0.2 V (SCE) in a solution of pH 14. This value shifts by about 25 mV per pH unit which implies that the redox reaction is a two electron process. After etching the crystal in H_2O_2 or after a few days of electrochemical experiments this phenomenon disappears.

In summary, the reduction wave occurs both in the light and the dark, but only after cycling through the oxidation region. This implies that either the oxidation is reversible or that a species on the surface is being oxidized to form a species which is then reduced to a nonreactive form which remains on the surface or is desorbed. The fact that the phenomenon disappears with time or with H_2O_2 etching makes the latter presumption most plausible.

Despite the behavior of this unknown redox reaction the quantum efficiency for the

photodissociation of water for these materials does not change with time. The quantum efficiency is around 40% for these Nb-doped crystals at a bias of +0.5 V (SCE) with 370 nm illumination both before and after the waves at -0.2 V vs SCE are gone, which is more than twice that reported for most doped iron oxide materials (22, 23). A more quantitative photoelectrochemical study is in progress.

Conclusions

It has been shown that a homogeneous conducting corundum phase of Fe_2O_3 can be prepared by chemical vapor transport from the ternary solution of $\text{Fe}_{2-x}\text{Nb}_x\text{O}_3$ where $0 < x < 0.02$. Niobium-substituted Fe_2O_3 crystallizes with the corundum structure and is an n -type semiconductor which behaves well as an electrochemical anode for the photooxidation of water. The room temperature resistivity of $85 \Omega \text{ cm}$ for these crystals is significant since one of the barriers toward using iron oxide more successfully as a photoanode has been the high intrinsic resistivity of the undoped material. Magnetic susceptibility studies suggest that the conductivity of the samples arises from charge compensation resulting from reduction of iron(III) to iron(II) upon niobium substitution in the structure. Electrical measurements give an activation energy for the electron hopping of 0.22 eV.

The surfaces of these crystals have also been shown to be of the same composition as the bulk which emphasizes the homogeneity of the material. Compositional analysis by Auger electron spectroscopy indicates that there is a layer of carbon on the surface which is easily removed by argon ion bombardment. Most important is the fact that we can obtain a LEED pattern from these single crystals directly after preparation. The hexagonal LEED pattern observed agrees with the bulk X-ray diffraction data showing that the crystals have

grown in the orientation of the (001) face of the corundum structure. XPS data show that the concentration of Nb at the surface is on the same order as that in the bulk, i.e., that there is no surface segregation of the Nb. The O/Fe ratio from XPS is also indicative of the Fe_2O_3 phase.

The large size of these crystals combined with the homogeneity of the surface and bulk makes these materials a good prototype for studying catalytic or simulated electrochemical reactions in an ultra high vacuum chamber. The photoanode behavior of the Nb-doped crystals competes well both qualitatively and quantitatively with doped polycrystalline samples. Because these crystals are very homogeneous, while sintered polycrystalline materials are usually not, these single crystals can be used to understand the fundamental processes (mechanisms) for a variety of reactions.

Acknowledgments

This work was supported by the Director, Office of Energy Research, Office of Basic Energy Sciences, Chemical Sciences Division of the U. S. Department of Energy under Contract DE-AC03-76SF00098. C.S. acknowledges support from the National Science Foundation under Grant INT/8412371. The authors acknowledge the cooperation of Dr. R Kershaw from A. Wold laboratories at the Brown University Materials Research Department for performing the measurements of electrical resistivity versus temperature, and Dr. N. Edelstein and G. Shalinoff for their assistance with the magnetic measurements on the "SQUID" susceptometer in the Materials and Molecular Research Division of Lawrence Berkeley Laboratory.

References

1. D. CORNACK, R. F. GARDNER, AND R. L. MOSS, *J. Catal.* **17**, 219 (1970).
2. R. SHINAR AND J. H. KENNEDY, *Solar Energy Mater.* **6**, 323 (1982).
3. W. H. STREHLOW AND E. L. COOK, *J. Phys. Chem.* **2**, 163 (1973).
4. F. P. KOFFYBERG, K. DWIGHT, AND A. WOLD, *Solid State Commun.* **30**, 1735 (1979).
5. R. F. GARDNER, F. SWEET, AND D. W. TANNER, *J. Phys. Chem. Solids* **24**, 1183 (1963).

6. B. M. WARNES, F. F. APLAN, AND G. SIMKOVICH, *Solid State Ionics* **12**, 271 (1984).
7. J. B. GOODENOUGH, in "Progress in Solid State Chemistry" (H. Reiss, Ed.), Vol. 5, p. 145, Pergamon, New York (1971).
8. J. H. KENNEDY AND K. W. FREESE, JR., *J. Electrochem. Soc.* **125**, 723 (1978).
9. G. HOROWITZ, *J. Electroanal. Chem.* **159**, 421 (1983).
10. K. D. SIEBER, C. SANCHEZ, J. E. TURNER, AND G. A. SOMORJAI, *J. Chem. Soc. Faraday Trans. 1* **81**, 1263 (1985).
11. L. J. VAN DER PAUW, *Phillips Res. Rep.* **13**, 9 (1958).
12. P. MERCHANT, R. COLLINS, K. DWIGHT, AND A. WOLD, *J. Solid State Chem.* **27**, 307 (1979).
13. V. AGAFONOV, D. MICHEL, M. PEREZ Y JORBA, AND M. FEDOROFF, *Mater. Res. Bull.* **19**, 233 (1984).
14. A. C. TURNOCK, *J. Amer. Ceram. Soc.* **49**, 177 (1966).
15. E. F. BERTAUT, L. CORLISS, F. FORRAT, R. ALEONARD, AND R. PAUTHENET, *J. Phys. Chem. Solids* **21**, 234 (1961).
16. G. H. GEIGER AND J. B. WAGNER, JR., *Trans. Metallurgical Soc. AIME* **233**, 792 (1965).
17. H. J. VANDAAL AND A. J. BOSMAN, *Phys. Rev.* **158**, 736 (1961).
18. K. D. SIEBER, C. SANCHEZ, J. E. TURNER, AND G. A. SOMORJAI, *Mater. Res. Bull.* **20**, 153 (1985).
19. M. SEO, J. B. LUMSDEN, AND R. W. STAEBLE, *Surf. Sci.* **50**, 541 (1975).
20. K. L. HARDEE AND A. J. BARD, *J. Electrochem. Soc.* **124**, 215 (1977).
21. C. LEYGRAF, M. HENDEWERK, AND G. A. SOMORJAI, *J. Catal.* **78**, 314 (1982).
22. R. K. QUINN, R. D. NASBY, AND R. J. BAUGHMAN, *Mater. Res. Bull.* **11**, 1011 (1976).
23. M. T. DARE-EDWARDS, J. B. GOODENOUGH, A. HAMMETT, AND P. R. TREVELLICK, *J. Chem. Soc. Faraday Trans. 1* **79**, 2027 (1983).